Latin American Journal of Solids and Structures
www.lajss.org

Optimum dynamic analysis of 2D frames using free-scaled wavelet functions

Abstract
This paper presents a wavelet-based scheme for dynamic analysis of 2-dimensional (2D) frames. In the proposed approach, free-scaled wavelet functions are developed for Multi-Degrees-of-Freedom (MDOF) structures, particularly, complex Chebyshev and simple Haar wavelets are implemented. A simple step-by-step and explicit algorithm is presented to calculate the time history response of 2D frames. The validity of the proposed procedure is demonstrated with two examples compared with several common numerical integration procedures such as family of Newmark-β, Wilson-θ and central difference method. Finally, it is shown that dynamic analysis of 2D frames is optimally accomplished by lesser computational time and high accuracy of results.

Keywords
Optimum structural dynamics, explicit integration method, numerical approximation, free-scaled wavelet functions, Chebyshev wavelet, Haar wavelet.

S.H. Mahdavi [a]
H.A. Razak [b]

[a] StrucHMRS Group, Department of Civil Engineering, University of Malaya, 50603 Kuala Lumpur, Malaysia; E-mail: s.h.mahdavii@gmail.com
[b] StrucHMRS Group, Department of Civil Engineering, University of Malaya, 50603 Kuala Lumpur, Malaysia; E-mail: hashim@um.edu.my

1 INTRODUCTION

In general, step-by-step time integration methods are being widely considered for the solution of the second-ordered differential equation of motion. For this case, researchers are more interested to a powerful and precise numerical integration scheme, particularly, for the solution of Multi-Degrees-of-Freedom (MDOF) systems. Bathe (1996) and Chopra (1995) presented that time integration approaches are the most capable schemes for either the nonlinear dynamic analysis or time history evaluation of large-scaled systems (Wilson *et al.*, 1973).

According to Bathe (1996), Chung (1994) and Huges (1987), numerical integration approaches are being categorized into the two basic categories. One is explicit scheme and other one is implicit procedure. An approach will be explicit provided that the equation of motion of the current time step is not utilized for determination of the current step displacement while will be implicit if it is involved. On the other hand, there are another two divisions. First, direct integration methods whereby the quantities of the dynamic system are being calculated through a direct space vector in the step-by-step solution of equation of motion. Secondly, indirect time integration schemes involving all corresponding equations being numerically transformed into a new space vector. For example, Fourier transformation has been introduced as a well-known and indirect integration scheme although with a major shortcoming that will be discussed later (Dokainish and Subbaraj, 1989). In addition, Chang (2002, 2010) reported that the considerable advantage of explicit methods is that it is unnecessary to solve a system of equations or there is no need to use a particular pre-starting scheme to commence solving a problem. For this reason, an explicit method is generally preferred over an implicit method in performing structural dynamics while it can be implemented quite easy

and requires low storage capacity. Furthermore, regarding to Rio *et al.* (2005), Torii and Machado (2012), Wilson *et al.* (1973), Chang (2010), since the practice of an explicit method is much simpler than implicit method for solution of dynamic or pseudo-dynamic tests, several explicit schemes have been improved for not only framed but also Finite Element structural dynamics, shock and wave propagation problems.

Nowadays, considerable researches are devoted to practice of wavelet analysis in various fields of science and engineering. Several attractive characteristics of wavelets such as efficient multi-scale decomposition, localization problems in physical and wave-number spaces and the existence of recursive and fast wavelet transforms, have obtained practice of this efficient method for the numerical solution of not only ordinary differential equations (ODEs) but also partial differential equations (PDEs) (Mahdavi and Shojaee, 2013).

Lepik (2005, 2008, 2009), Babolian and Fatahzadeh (2010) and Yuanlu (2010), have implemented the wavelet analysis for solution of ordinary and fractional differential equations. All of them have considered wavelet analysis to examine equations under different constraints. For instance, solution of time dependent equations being constrained only in a unit time interval. In addition, there is no attention addressed on magnitude and qualification of various natural frequencies corresponding to the frequency content of external excitation. Although, practice of several filter banks has been presented by Salajeghe and Heidari (2006); the time integration process has not been improved yet.

Cattani (2004) and Babolian and Fatahzadeh (2010) reported that, the signal is evaluated based on its frequency content through the wavelet analysis. This is being accomplished by shifting the wavelet window along the time axis in the neighborhood of the current window and relies on a time-scaled-frequency analysis. As a result, all information in the time domain remains. In contrast, the Fourier transforms (FT), that the information is lost along the time domain.

Fundamentally, the efficiency of numerical procedures is more considered in the case of dynamic analysis of MDOF systems e.g., 2D frames or trusses (El-Sheikh, 2000 and Liu, 2002). Implementation of the simple Haar wavelet for the numerical solution of dynamic responses of Single-Degree-of-Freedom (SDOF) systems has been recently presented by Mahdavi and Shojaee (2013). They found that even simple Haar wavelet function gains very optimal and accurate results for the SDOF structures and also they recommended to improve the proposed approach on MDOF structures and to utilize a complex basis function of wavelet i.e., Chebyshev wavelet function. In this study, the proposed method is generated for solution of MDOF structures using two different types of wavelet functions such as free-scaled complex Chebyshev wavelet and simple Haar wavelet functions.

This paper is organized as follows. In the next section a brief review of simple Haar wavelet functions and complex Chebyshev wavelet functions is presented. Section 3 is allocated to implementation of the wavelet function on solution of dynamic analysis of MDOF systems. For this purpose, a comprehensive procedure is proposed to utilize any wavelet function. Section 4 is devoted to investigation of the validity and effectiveness of the proposed method on two applications.

2 BRIEF REVIEW ON WAVELET ANALYSIS

2.1 Haar wavelet functions

Haar basis function was presented by Alfred Haar in 1910. The simple family of Haar wavelet for $t \in [0,1]$ is shown by $h_{m-1}(t)$ (Mahdavi and Shojaee, 2013):

$$h_i(t) = 1 \ \ if \ \ t \in \left[\frac{b}{m}, \frac{b+0.5}{m}\right] \ \ or \ \ h_i(t) = -1 \ if \ t \in \left[\frac{b+0.5}{m}, \frac{b+1}{m}\right] \ or \ h_i(t) = 0 \ \ otherwise \tag{1a}$$

where;

$$i = m + b + 1 \tag{1b}$$

where, integer $m = 2^j (j = 0, 1, \dots, J)$ shows the order of wavelet; J is maximum level of the resolution, $b = 0, 1, \dots, m-1$ indicates the parameter of transition. According to the Segmentation Method (SM) content of a function is simplified and changed into the new domain that is entirely appropriate to analysis through the applied approach. In this study, $2M$ denotes the number of segmentations in each global time interval regarding to the scale of proposed wavelet. Accordingly, maximum value of $i = 2M = 2^{J+1}$ (Lepik, 2005).

Function $f(t)$ may be approximated in Haar series as (Mahdavi and Shojaee, 2013):

$$f(t) \cong \sum_{i=0}^{2M} c_i h_i(t) \tag{2a}$$

In consequence, Haar coefficients c_i $(i = 0, 1, 2, \dots)$ are calculated by:

$$c_i = 2^j \int_0^1 f(t)\, h_i(t) dt \tag{2b}$$

Hence, through algebraic calculations, Haar coefficients are given directly as follows:

$$c_i = f(t) H_{2M}^{-1}(t) \tag{2c}$$

H_{2M} is a square matrix $(2M \times 2M)$, including, the first $2M$ scaled of Haar wavelet. Equivalently, function $f(t)$ may be rewritten as follows:

$$f(t) \cong c_{2M}^T H_{2M}(t) \tag{3}$$

For the sake of algebraic approximation, integration of H_{2M} is obtained by Haar series with new square coefficient matrix of P_{2M} as following (Lepik, 2005):

$$\int_0^1 H_{2M}(t) dt \approx P\, H_{2M}(t) \tag{4}$$

According to the Segmentation Method local times are calculated relatively to the scale of wavelet as (Mahdavi and Shojaee, 2013):

$$\tau_l = \frac{l - 0.5}{2M}, \qquad l = 1, 2, \dots, 2M \tag{5a}$$

Subsequently, the local computation time (τ_l), is obtained as:

$$t_{lt} = d_t(\tau_l) + t_t \Rightarrow \tau_l = \frac{t_t - t_{lt}}{d_t}, \qquad l = 1,2, \dots, 2M \tag{5b}$$

Consequently, the coefficient matrix of wavelet is derived corresponding to local computation time i.e., $H(i, l) = h_i(t_l)$ for Haar wavelet. Definition of the operation matrix of the integration (P) and coefficient matrix of Haar (H) are shown in a study conducted by Mahdavi and Shojaee (2013).

2.2 Chebyshev wavelet functions

The general expression for Chebyshev polynomials, the first (T_n) and the second kind (U_n) are defined as follows (Integer n indicates order of polynomial) (Fox and Parker, 1968):

$$T_n(x) = \left(\frac{n}{2}\right) \sum_{k=0}^{n/2} \left((-1)^k \frac{(n-k-1)!}{(n-2k)!\, k!} \times (2x)^{n-2k}\right), \quad n = 1, 2, 3, \dots \tag{6a}$$

$$U_n(x) = \sum_{k=0}^{n/2} \left((-1)^k \frac{(n-k)!}{(n-2k)!\, k!} \times (2x)^{n-2k}\right), \quad n = 1, 2, 3, \dots \tag{6b}$$

The variable weight functions of $T_n(x)$ and $U_n(x)$ are obtained as $\omega_{(x)}$using Eqs. (7a) and (7b), respectively (Mason and Handscomb, 2003):

$$\omega_{T_n}(x) = \begin{cases} 1/\sqrt{1-x^2} & |x| < 1 \\ 0 & |x| \geq 1 \end{cases} \tag{7a}$$

$$\omega_{U_n}(x) = \begin{cases} (2/\pi)\sqrt{1-x^2} & |x| < 1 \\ 0 & |x| \geq 1 \end{cases} \tag{7b}$$

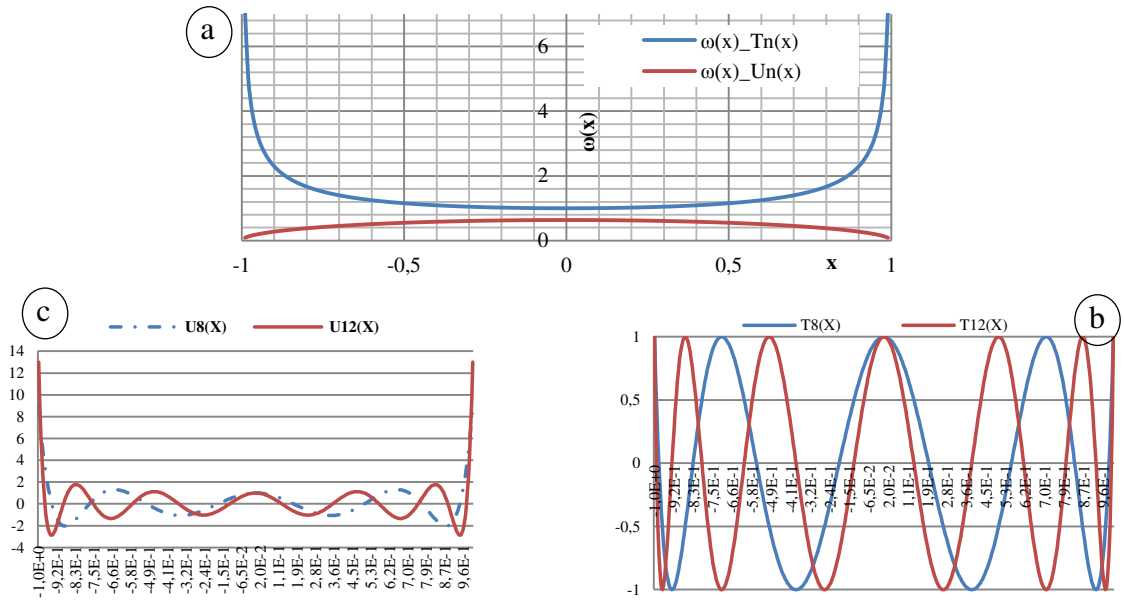

Figure 1. (a) Weight functions, (b) shape functions for the 8th and 12th order, (c) shape functions for the 8th and 12th order, corresponding to the first ($T_n(x)$) and second (($U_n(x)$) kind of Chebyshev polynomials.

According to Figure 1a and Eq. (7), orthogonality of Chebyshev polynomials is satisfied using described weight functions for the both kinds. In addition, Figures 1b and 1c illustrate shape functions of the first and second kind of Chebyshev polynomials, namely $T_n(x)$ and $U_n(x)$, corresponding to the 8th and 12th orders, respectively.

In this paper the first kind of Chebyshev polynomials are discussed. Accordingly, Chebyshev wavelet refers to the first one (Eq. (6a)). In addition, Chebyshev wavelet arguments are defined by (Babolian and Fatahzadeh, 2010 and Yuanlu, 2010):

$$\Psi_{n,m} = \Psi(k,n,m,t)\,,\ n = 1,2,\dots,2^{k-1}\,,\ m = 0,1,\dots,M-1\,,\ k = 1,2,3,\dots \tag{8}$$

where, k shows the factor of transition and it is assumed any positive integer, t denotes the time, m is the degree of Chebyshev polynomials for the first kind and n denotes the considered scale of wavelet. Subsequently, Chebyshev wavelets are constructed with substituting the first kind (T_n) with relevant weight function for each scale and transition, in the wavelet definition:

$$\psi_m(t) = \begin{cases} (2^{k/2}) \times T_m(2^k(t) - 2n + 1), & \frac{n-1}{2^{k-1}} < t \leq \frac{n}{2^{k-1}} \\ 0 & \textit{Otherwise} \end{cases} \tag{9}$$

where T_m in Eq. (9) is calculated as follows:

$$T_m(t) = \begin{cases} 1/\sqrt{\pi} & m = 0 \\ T_m \times \sqrt{\dfrac{2}{\pi}} & m > 0 \end{cases} \tag{10}$$

Hence, the weight functions are obtained as:

$$\omega_n(t) = \omega(2^k.t - 2n + 1) \tag{11}$$

To utilize Chebyshev wavelet through the SM method, if D is assumed as the number of segmentation in global time, M will be the order of Chebyshev polynomials, obtained as follows:

$$2^{k-1}M = D \Longrightarrow M = D/2^{k-1} \tag{12}$$

Furthermore, Eq. (2a) is rewritten by Chebyshev wavelet as (Babolian and Fatahzadeh, 2010):

$$f(t) \approx \sum_{n=1}^{2^{k-1}} \sum_{m=0}^{M-1} C_{n,m}\psi_{n,m}(t) = C^T.\psi(t) \tag{13}$$

where, vector of $C_{n,m}$ shows the coefficient matrix of Chebyshev and the vector of the Chebyshev operation matrix is designed by $\psi_{n,m}(t)$ as (Yuanlu, 2010):

$$C = [c_1, c_2, c_3, \dots, c_{2^{k-1}}]^T_{2^{k-1}M\times 1} \quad \Leftrightarrow \quad C_i = [c_{i0}, c_{i1}, c_{i2}, \dots, c_{i,M-1}]^T \tag{14}$$

$$\psi(t) = [\psi_1, \psi_2, \psi_3, \dots, \psi_{2^{k-1}}]^T_{2^{k-1}M\times 1} \quad \Leftrightarrow \quad \psi_i(t) = [\psi_{i0}(t), \psi_{i1}(t), \psi_{i2}(t), \dots, \psi_{i,M-1}(t)]^T \tag{15}$$

In addition, the local times τ_l in the SM method are calculated as follows:

$$\tau_l = \left({}^{1}/_{2^{k-1}M}\right)(l - 0.5) \quad , \; l = 1, 2, 3, \dots, 2^{k-1}M \tag{16}$$

Accordingly, a $2^{k-1}M \times 2^{k-1}M$-dimensional square matrix of $\phi_{n,m}(t)$ is obtained as (Yuanlu, 2010):

$$\phi_{n,m}(t) = [\psi(t_1)\ \psi(t_2)\ \dots\ \psi(t_i)]_{2^{k-1}M\times 2^{k-1}M} \tag{17}$$

In addition, Babolian and Fatahzadeh (2010) and Yuanlu (2010), presented the definition of the operation matrix of the integration (P) and coefficient matrix of Chebyshev ($\phi_{n,m}(t)$).

3 IMPLEMENTATION OF WAVELET SCHEME ON MDOF SYSTEMS

Numerically, second derivation (acceleration) of each degree of freedom for a 2D frame system i.e., rotational (θ), axial (u) and shear (y), can be shown as Eq. (3) for Haar wavelet or Eq. (13) for Chebyshev wavelet, as follows:

$$\begin{aligned} \ddot{u}(t) &= C_1^T \times \psi(t) \\ \ddot{y}(t) &= C_2^T \times \psi(t) \\ \ddot{\theta}(t) &= C_3^T \times \psi(t) \end{aligned} \tag{18}$$

Using Eq. (4) the first order of derivation (velocity), for each degree of freedom (DOF) is approximated, multiplying by operation of integration (P), as follows (will be applied for 3 degrees of freedom):

$$\begin{aligned} \dot{u}(t) &= C_1^T \times P \times \psi(t) + \dot{u_n} \\ \dot{y}(t) &= C_2^T \times P \times \psi(t) + \dot{y_n} \\ \dot{\theta}\,(t) &= C_3^T \times P \times \psi(t) + \dot{\theta_n} \end{aligned} \tag{19}$$

where, $\dot{u}_n$, $\dot{y}_n$ and $\dot{\theta}_n$ are initial velocity regarding to the axial, shear and rotational DOFs, respectively. Next, using Eq. (4), quantities of displacement in x and y directions and rotation are numerically approximated as follows:

$$\begin{aligned} u(t) &= C_1^T \times P^2 \times \psi(t) + u_n \\ y(t) &= C_2^T \times P^2 \times \psi(t) + y_n \\ \theta(t) &= C_3^T \times P^2 \times \psi(t) + \theta_n \end{aligned} \tag{20}$$

To solve above equations, initial calculation corresponding to each DOF should be approximated by relative wavelet functions (u_n, y_n and θ_n). For this purpose, the unity is being expanded by the Chebyshev wavelet as:

$$1 \cong I^* \times \psi(t) \cong \left(\sqrt{\pi}/_2\right) \times [1,0,0,\dots,1,0,0,\dots] \times \psi(t) \tag{21a}$$

Alternatively, for the Haar wavelet, it is being obtained as:

$$1 \cong I^* \times h(t) \cong [1,0,0,\dots,0,0,0,\dots] \times h(t) \tag{21b}$$

where, Eqs. (21a) and (21b) refer to the dependent vectors that make the coefficient matrix of specific wavelet to be unity. For example, for each particular wavelet, it should be calculated individually. Hence, initial calculations of velocity and displacements for three DOF are developed as:

$$\begin{aligned} \dot{u}_n &= N_{1-1}^T \times \psi(t) \\ \dot{y}_n &= N_{1-2}^T \times \psi(t) \\ \dot{\theta}_n &= N_{1-3}^T \times \psi(t) \end{aligned} \tag{22a}$$

$$\begin{aligned} u_n &= N_{2-1}^T \times \psi(t) \\ y_n &= N_{2-2}^T \times \psi(t) \\ \theta_n &= N_{2-3}^T \times \psi(t) \end{aligned} \tag{22b}$$

where, N_{1-i}^T and N_{2-i}^T are $2^{k-1}M \times 1$ dimension vectors corresponding to the i th DOF, that are similarly obtained by Chebyshev wavelet, as follows:

$$N_1^T \cong v_{n(0)} \times \left(\sqrt{\pi}/_2\right) \times [1,0,0,\dots,1,0,0,\dots]^T \tag{22c}$$

$$N_2^T \cong u_{n(0)} \times \left(\sqrt{\pi}/_2\right) \times [1,0,0,\dots,1,0,0,\dots]^T \tag{22d}$$

Substituting Eq. (22) into Eqs. (19) and (20), quantities of velocity and displacement are numerically obtained for each DOF, as follows (e.g., for axial DOF):

$$\dot{u}(t) = C_1^T \times P \times \psi(t) + N_{1-1}^T \times \psi(t) \tag{23a}$$

$$u(t) = C_1^T \times P^2 \times \psi(t) + N_{1-1}^T \times P \times \psi(t) + N_{2-1}^T \times \psi(t) \tag{23b}$$

Next, $F(t)$ is approximated with various scale of the proposed wavelet function as follows:

$$F(t) = f^T \times \psi(t) \tag{24a}$$

where, the applied time history force $F(t)$ is $1 \times 2^{k-1}M$ vector, contains a set of separate values related to the local times (Eqs. (5) and (16)). Consequently, the coefficient matrix of load is numerically obtained by:

$$f_{1\times 2^{k-1}M}^T = F_{1\times 2^{k-1}M} / \phi_{(2^{k-1}M)\times(2^{k-1}M)} \tag{24b}$$

Theoretically, dynamic equilibrium governing the linear time history responses of a multi-degrees-freedom system (MDOF) is expressed as:

$$M^*.\ddot{U}_t + C^*.\dot{U}_t + K^*.U_t = F_t \tag{25}$$

where, M^*, $C^*$and K^* indicate the mass, damping and stiffness matrix of MDOF system, respectively; vector F_t is the externally applied load; $\ddot{U}_t$, $\dot{U}_t$ and U_t contain acceleration, velocity and displacement vectors corresponding to each DOF on discrete set of SM point of local time. On the other word, provided that d and $2M$ are assumed as DOF and order of the wavelet (related to the selected scale of wavelet) respected to the MDOF system, dimension of acceleration, velocity and displacement matrix are determined as $d \times 2M$ where characteristic matrix of system are determined by $d \times d$ matrixes of M^*, $C^*$and K^*. According to previous derivations, dynamic equilibrium will be relatively rewritten by its wavelet components as follows:

$$\begin{aligned} M^*.\begin{bmatrix} C_1^T \times \psi(t) \\ \vdots \\ C_d^T \times \psi(t) \end{bmatrix}_{d\times 2M} + C^*.d_t.\begin{bmatrix} C_1^T \times P \times \psi(t) + N_{1-1}^T \times \psi(t) \\ \vdots \\ C_d^T \times P \times \psi(t) + N_{1-d}^T \times \psi(t) \end{bmatrix}_{d\times 2M} + \\ K^*.d_t^2.\begin{bmatrix} C_1^T \times P^2 \times \psi(t) + N_{1-1}^T \times P \times \psi(t) + N_{2-1}^T \times \psi(t) \\ \vdots \\ C_d^T \times P^2 \times \psi(t) + N_{1-d}^T \times P \times \psi(t) + N_{2-d}^T \times \psi(t) \end{bmatrix}_{d\times 2M} - d_t^2.\begin{bmatrix} f_1^T \times \psi(t) \\ \vdots \\ f_d^T \times \psi(t) \end{bmatrix}_{d\times 2M} \end{aligned} \tag{26}$$

To be noted that, d_t indicates the convertor of time from local time to the global time.

where, $\psi(t)$ is eliminated from both side of equation; Eq. (26) is simplified and rearranged to calculate unknown coefficient matrix of wavelet C_i^T related to each DOF as below:

$$\begin{aligned} &\begin{bmatrix} M_{11}^* & \dots & M_{1d}^* \\ \vdots & \ddots & \vdots \\ M_{d1}^* & \dots & M_{dd}^* \end{bmatrix}\begin{Bmatrix} C_1^T \\ \vdots \\ C_d^T \end{Bmatrix} + \begin{bmatrix} C_{11}^* & \dots & C_{1d}^* \\ \vdots & \ddots & \vdots \\ C_{d1}^* & \dots & C_{dd}^* \end{bmatrix}\begin{Bmatrix} C_1^T \times P + N_{1-1}^T \\ \vdots \\ C_d^T \times P + N_{1-d}^T \end{Bmatrix} \\ &+ \begin{bmatrix} K_{11}^* & \dots & K_{1d}^* \\ \vdots & \ddots & \vdots \\ K_{d1}^* & \dots & K_{dd}^* \end{bmatrix}\begin{Bmatrix} C_1^T \times P^2 + N_{1-1}^T \times P + N_{2-1}^T \\ \vdots \\ C_d^T \times P^2 + N_{1-d}^T \times P + N_{2-d}^T \end{Bmatrix} = \begin{bmatrix} f_1^T \\ \vdots \\ f_d^T \end{bmatrix} \end{aligned} \tag{27}$$

Expanding Eq. (27) as a vector for each row corresponding to each DOF (d) denoted by j, yields:

$$\sum_{i=1}^{d} M_{ji}^* C_i^T + \sum_{i=1}^{d} C_{ji}^* (C_i^T P + N_{1-i}^T) + \sum_{i=1}^{d} K_{ji}^* (C_i^T P^2 + N_{1-i}^T P + N_{2-i}^T) = f_j^T \tag{28}$$

where, j refers to each DOF from one to d. Next, Eq. (28) is factorized over C_i^T for i th row and simplified as follows (j is also particular DOF):

$$C_i^T\ (M_{ji}^* I + C_{ji}^* P + K_{ji}^* P^2) = f_j^T - \sum_{i=1}^{d} [C_{ji}^* N_{1-i}^T + K_{ji}^* (N_{1-i}^T P + N_{2-i}^T)] \tag{29a}$$

where, I denotes a $2M \times 2M$ identity matrix. The unknown coefficient wavelet vectors are calculated related to the dynamic equilibrium as:

$$\underbrace{\begin{bmatrix} S_{11} & \dots & S_{1(2M\times d)} \\ \vdots & \ddots & \vdots \\ S_{(2M\times d)1} & \dots & S_{(2M\times d)(2M\times d)} \end{bmatrix}}_{S} \underbrace{\begin{Bmatrix} \begin{Bmatrix} C_{11}^T \\ \vdots \\ C_{(2M)1}^T \end{Bmatrix} \\ \vdots \\ \begin{Bmatrix} C_{1d}^T \\ \vdots \\ C_{(2M)d}^T \end{Bmatrix} \end{Bmatrix}}_{B} = \underbrace{\begin{Bmatrix} \begin{Bmatrix} f_{11}^T \\ \vdots \\ f_{(2M)1}^T \end{Bmatrix} \\ \vdots \\ \begin{Bmatrix} f_{1d}^T \\ \vdots \\ f_{(2M)d}^T \end{Bmatrix} \end{Bmatrix} - \begin{Bmatrix} \{\sum_{i=1}^{d} [C_{1i}^* N_{1-i}^T + K_{1i}^* (N_{1-i}^T P + N_{2-i}^T)]\} \\ \vdots \\ \{\sum_{i=1}^{d} [C_{di}^* N_{1-i}^T + K_{di}^* (N_{1-i}^T P + N_{2-i}^T)]\} \end{Bmatrix}}_{R} \tag{29b}$$

where, $(2M \times d) \times (2M \times d)$ square matrix of S contains the whole characteristics of system i.e., effects of mass, damping and stiffness of structure. Accordingly, the first, second and the last $2M$ components of the first row in matrix S are computed as follows (using the left side of Eq. (29a)):

$$\begin{gathered} M_{11}^{*} I + C_{11}^{*} P + K_{11}^{*} P^{2} = S_{11} : S_{1(2M)} \\ M_{12}^{*} I + C_{12}^{*} P + K_{12}^{*} P^{2} = S_{1(2M+1)} : S_{1(2M\times 2)} \\ \vdots \\ M_{1d}^{*} I + C_{1d}^{*} P + K_{1d}^{*} P^{2} = S_{1(((d-1)\times 2M)+1)} : S_{1(2M\times d)} \end{gathered} \tag{30}$$

where, $S_{11}:S_{1(2M)}$ indicates columns of S_{11} to $S_{1(2M)}$. Furthermore, in Eq. (29b), B is a $(2M \times d)1$ vector, including d blocks of unknown coefficient vectors of wavelet, corresponding to each DOF. On the other hand of Eq. (29b), $(2M \times d)1$ vector of R is constructed from effects of initial conditions subtracting from the external load regarding to each DOF on collocation points.

Subsequently, coefficient vectors are calculated on each DOF using $[B] = [S]^{-1}[R]$. Eventually, relevant displacement, velocity and acceleration are calculated on nodes by Eq. (23).

4 NUMERICAL APPLICATIONS

In this section validity of the proposed method is examined through the evaluation of several results. Two applications are considered, including a small-scaled 2D frame under impact loads, and a large-scaled 2D frame under complex base excitation.

4.1 A 2D frame under impact loads

Figure 2 shows a 2D frame under two concentrated dynamic loads, including, one vertical force and one counter-wise moment. The system's characteristics and load time histories are shown in figure. Damping value is calculated proportionally as 0.01 percentage of stiffness. In addition to calculate time history responses, Δt—0.01 sec has been selected as time increment for common numerical approaches, while, Δt—0.05 sec has been utilized for the proposed method.

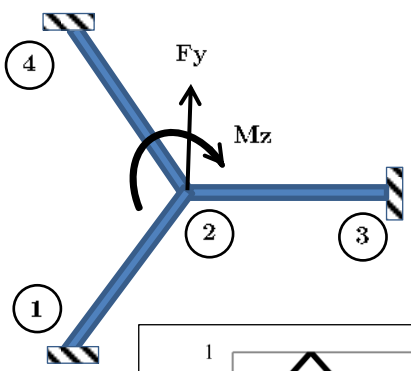

Node	Coordinates (cm) X	Y	
1	0	0	$\bar{m}$—0.02 kg/cm
2	50	100	E—210 GPa
3	150	100	A—6 cm^2
4	0	200	I—4.5 cm^4

Geometric and material properties

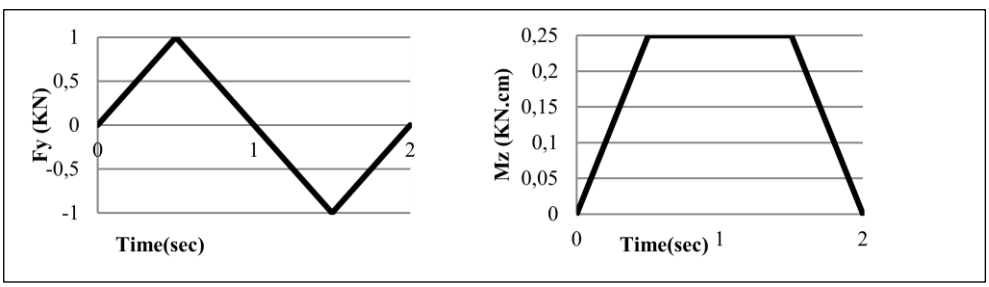

Figure 2. A 2D frame under concentrate impact loads.

The first 2 sec vertical displacements time history for the node 2 shown in Figure 2, were calculated with the proposed method including, 4th scale of (designated by 2M4) Haar wavelet (HA) and 4th and 16th scale of (designated by 2M4, 2M16) Chebyshev wavelet (CH) and common integration procedures including, central difference (CD), Wilson-θ (WIL) and exact method (results from Mode Superposition method using all modes are implied as analytical solution, namely exact method in this study), and plotted in Figure 3. This figure shows, the result calculated by the proposed method (particularly using Chebyshev wavelet) is closer to the exact solution than other considered numerical integration methods.

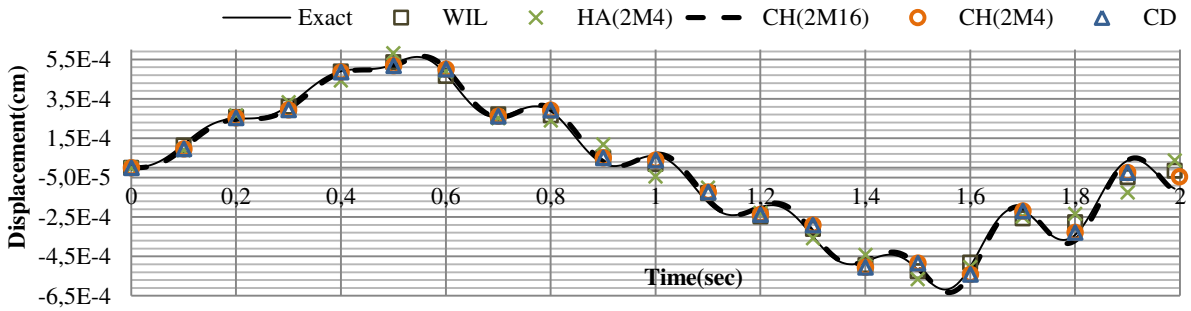

Figure 3. Vertical displacement time history of joint 2 shown in frame Figure 2.

To be noted that, percentile total average errors (PTAE) has been computed by assumption of $\propto$ for the measurement of exact responses and β for the responses calculated by each numerical integration approach (relative errors to each Z = time increments) as follows:

$$PTAE = (\sum_{i=0}^{Z} \frac{(\beta - \alpha) \times 100}{\alpha})/Z \tag{31}$$

To precisely evaluate the proposed method, total average errors and relative computational time are plotted in Figure 4. Note that dynamic analysis of current application is optimally achieved by using time increment of 0.05 sec for the proposed approach. Additionally, Figure 4 shows considerable percentile amount of error corresponding to the Haar wavelet compared with Chebyshev wavelet; although, from its optimization point of view it can be still considered for initial calculations. It is clearly distinguishable from this figure that, 16th scale of Chebyshev wavelet analyzed considered application more accurately and optimally.

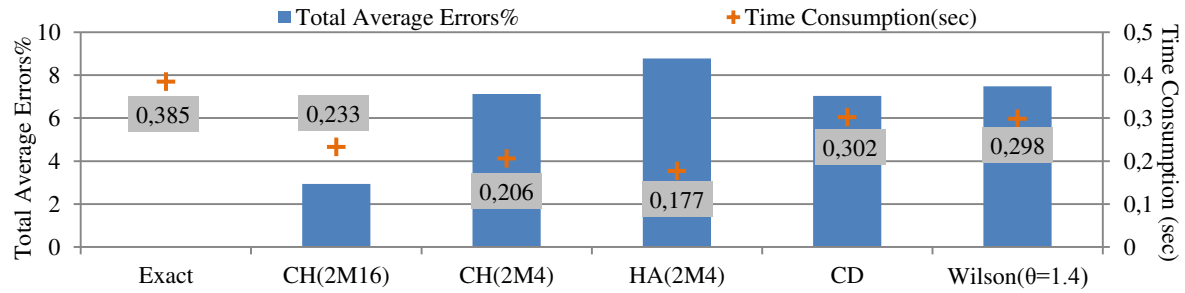

Figure 4. Total average errors in vertical displacement of joint 2, shown in Figure 2 and relative computation time involved (CH—Chebyshev, CD— central difference, HA—Haar).

Rotation time history of joint 2 shown in frame Figure 2 is plotted in Figure 5 for the first 2 second of loading. To be noted that, average acceleration of Newmark-β family (designated by AAc), has been also utilized to calculate responses of rotation. Finally, the total average error for the rotation time history analysis has been plotted in the Figure 6. For the further investigation, total computation time involved is shown in this figure with respect to each numerical scheme. The

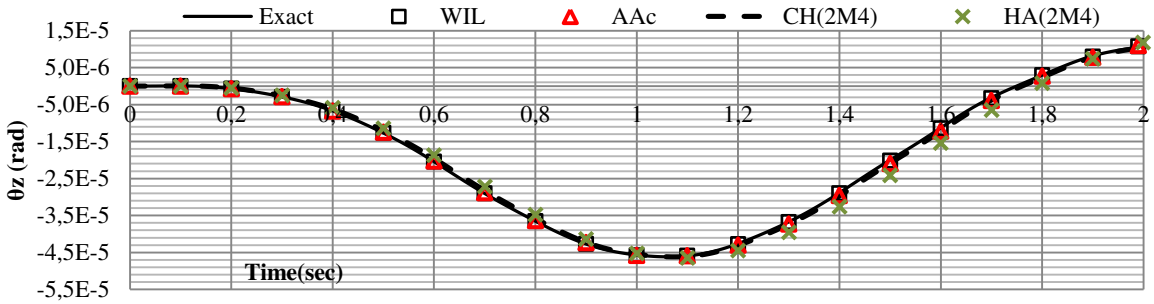

Figure 5. Rotation time history of joint 2 shown in frame Figure 2 (CH—Chebyshev, HA—Haar, AAc— average acceleration, WIL— Wilson-θ).

efficiency of the proposed scheme is apparent from Figures 5 and 6, particularly when a low scale of Chebyshev wavelet has been utilized. However, it is theoretically concluded that accurate dynamic analysis is achieved by using the large scale of wavelet functions. In practice, it is observed that, to achieve the optimal dynamic analysis, the scale of corresponding wavelet function is directly related to the frequency content of applied loading. For instance, in this application, it was inferred that dynamic analysis of the structure is optimally achieved by a low scale of an efficient basis function facing with smooth types of loadings.

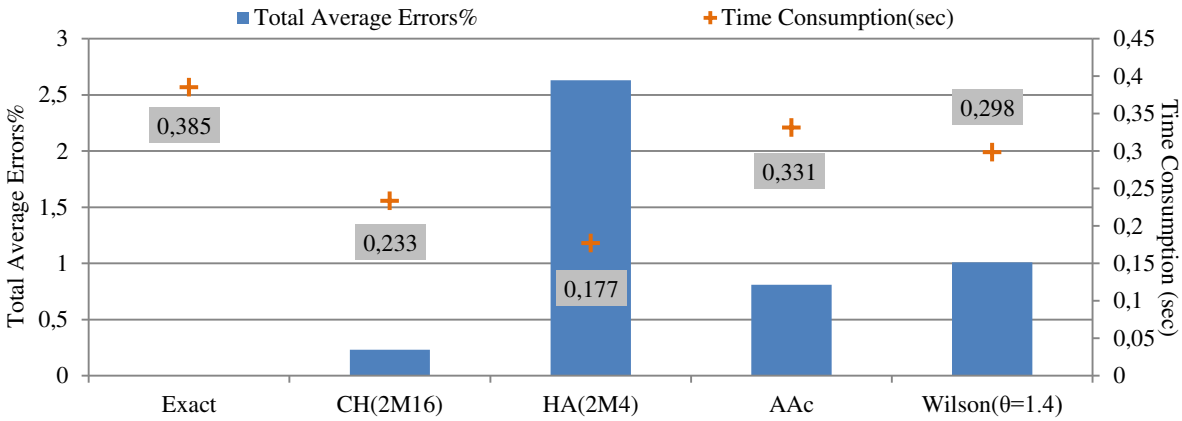

Figure 6. Total average errors in rotation of joint 2, shown in Figure 2 and relative computation time involved (CH—Chebyshev, HA—Haar, AAc—average acceleration).

4.2 A large-scaled 2D frame under complex ground acceleration

Figure 7 shows a 2D large-scaled frame subjected to the El-Centro base acceleration. All frame's characteristics have been chosen the same and shown in figure. In addition, damping ratio is assumed proportionally 0.01 percentages of stiffness. Furthermore, minimum period of this system was calculated as T_{min}—0.01046 sec thus, at least $\Delta t \leq 0.55T_{min}$— 0.00575 sec (Bathe, 1996 and Hughes, 1987) has been utilized as time increment for common integration schemes, particularly, to gain stability of responses those computed by central difference method. It is to be noted that Δt—0.05 and 0.01 sec is selected for the proposed approach and common numerical schemes, respectively.

This problem is evaluated by using five numerical procedures which includes, central difference, Wilson (θ—1.4), linear acceleration from family of Newmark-β (designated by LA), the proposed method using 8th scale of Haar (designated by HA(2M8)) and 8th scale of Chebyshev wavelet (designated by CH(2M8)), and comparing with the piecewise modal Duhamel integration (supposedly the exact solution).

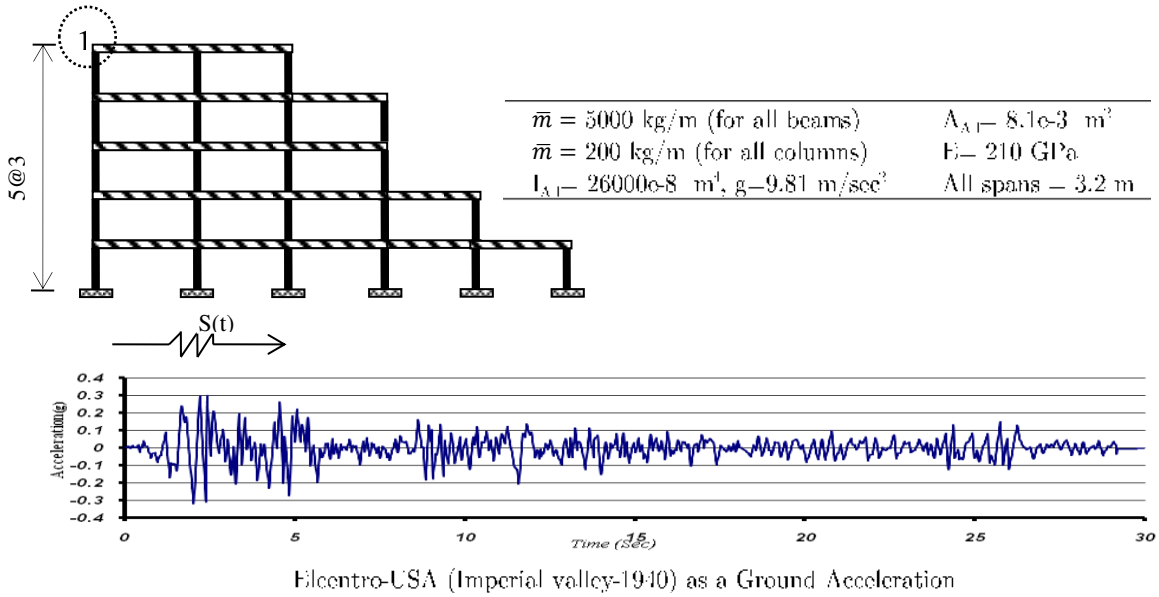

Elcentro-USA (Imperial valley-1940) as a Ground Acceleration

Figure 7. A large-scaled 2D frame under broad-frequency content ground acceleration.

Figure 8 shows the first 10 sec horizontal time history displacements of node 1 shown in Figure 7. It can be clearly deduced from the figure that the accuracy of results calculated by the 8th scale of Chebyshev wavelet, while most of the time gave the highest value. Furthermore, this figure illustrates that responses computed by Haar wavelet are almost undesirable. Theoretically, the shortcoming of Haar wavelet is because of two reasons. Firstly, the point of discontinuity located at node 0.5 (Eq. (1)) in the inherent shape function of Haar wavelet. Secondly, inaccurate approximation of wide-frequency-content excitation compared with accurate approximation of 8th scale of Chebyshev wavelet known as low-scaled.

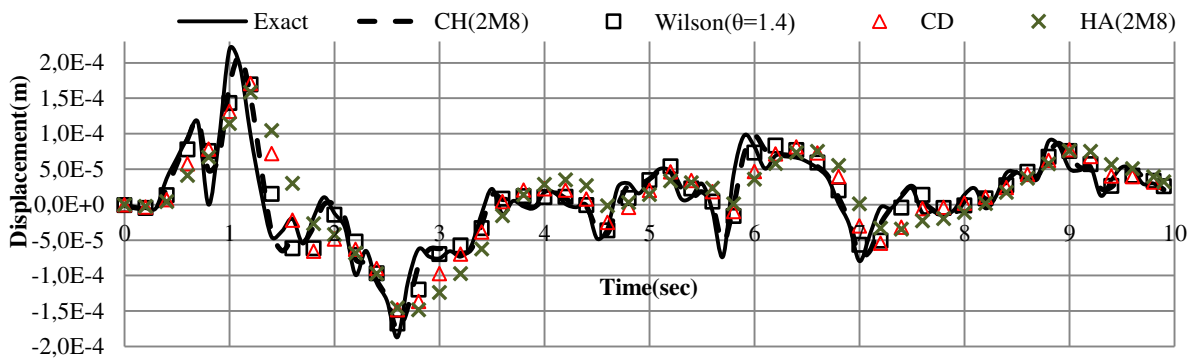

Figure 8. The first 10 sec horizontal displacement time history of joint 1 shown in frame Figure 7 (CH—Chebyshev, CD— central difference, HA—Haar).

For the purpose of comparison, the first 3 sec horizontal time history displacements of node 1 shown in Figure 7 have been plotted in Figure 9. It is clearly deduced from figure that results computed by linear acceleration from family of Newmark-β (known as an explicit method) are almost near to Wilson-θ; although, with lesser errors.

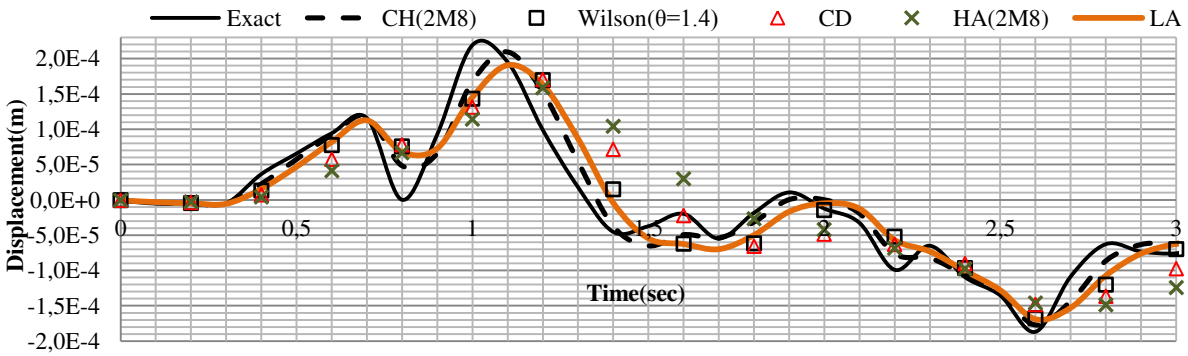

Figure 9. The first 3 sec horizontal displacement time history of joint 1 shown in frame Figure 7 (CH—Chebyshev, CD— central difference, HA—Haar, LA—linear acceleration).

Eventually, the total average error and computation time involved is plotted in Figure 10, corresponding to the first 10 sec of excitation. As can be seen from figure, the results computed by Haar wavelet, significantly returned the highest value of 80.08% (total average error). As a reason, external excitation with broad-frequency contents is not being accurately approximated with simple Haar wavelet functions. In addition, the computational time was the lowest at 0.991 sec compared with 1.402 sec for a low scale of Chebyshev wavelet or 1.974 sec for central difference method. However, Figure 10 illustrates that the exact solution gave a computational time of 2.65 sec without errors but it should be noted that this is applicable for only small-scaled structures. Consequently, this figure also illustrates the efficiency of the 8th scale Chebyshev wavelet which is sufficiently accurate to compute broad-frequency-content loading for this particular problem, in comparison with the other numerical procedures. Overall, from the optimization point of view, it can be concluded that responses calculated by Haar wavelet may be considered for purposes of initial evaluation.

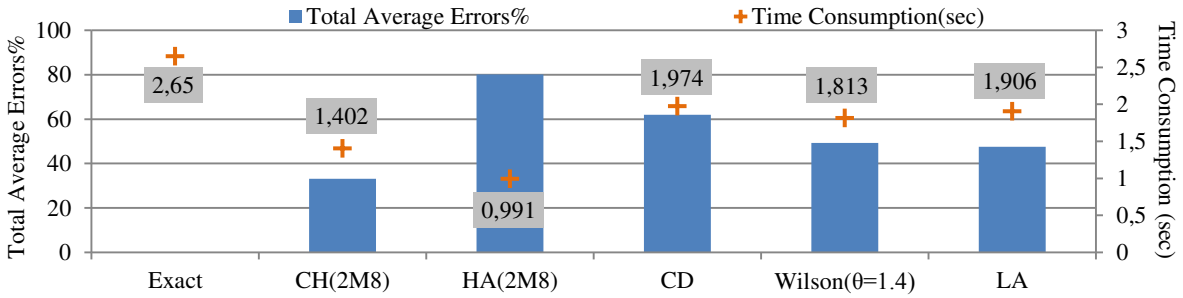

Figure 10. Total average errors in displacement of joint 1, shown in Figure 7 and relative computation time (CH—Chebyshev, CD— central difference, HA—Haar, LA—linear acceleration).

5 CONCLUSIONS

This paper presents a new explicit indirect time integration scheme to calculate the time history response of 2D frames using free scale of wavelet functions. It is shown that result from utilizing the proposed approach to solve second-ordered differential equation of motion is optimally being calculated through a clear cut formulation with a simple algorithm for linear dynamic analysis. According to the comprehensive formulations which were presented, a compatible dynamic analysis will be accomplished by practice of several wavelet basis functions. In addition, it is deduced that the proposed method is accurate and fast to analyze. This procedure can be simply generalized for large-scaled and nonlinear systems; although, in this paper just the linear problems have been discussed to establish and introduce a new methodology.

Acknowledgement

The authors would like to express their sincere thanks to University of Malaya (UM) and the Ministry of Higher Education (MOHE), Malaysia for the support given through research grants FP027/2012A and UM.C/625/1/HIR/MOHE/ENG/55.

References

Babolian, B., Fatahzadeh, F. (2010). Numerical solution of differential equations by using Chebyshev wavelet operational matrix of integration. Applied Mathematics and Computations 188:417-426.

Bathe, K.J. (1996). Finite Element Procedures, Prentice-Hall, Englewood Cliffs (New Jersey).

Cattani, C. (2004). Haar wavelets based technique in evolution problems. Proc. Estonian Academy of Sciences, Physics, Math. 53(1):45-63.

Chang, S.Y. (2002). Explicit pseudo-dynamic algorithm with unconditional stability. Journal of Engineering Mechanics (ASCE) 128(9):935-947.

Chang, S.Y. (2010). A new family of explicit methods for linear structural dynamics. Computers and Structures 88:755-772.

Chopra, A.K. (1995). Dynamic of Structures: Theory and Applications to Earthquake Engineering, Prentice-Hall, Englewood Cliffs (New Jersey).

Chung, J., Lee, J.M. (1994). A new family of explicit time integration methods for linear and non-linear structural dynamics. International Journal of Numerical Methods in Engineering 37:3961-3976.

Dokainish, M.A., Subbaraj, K. (1989). A survey of direct time integration methods in computational structural dynamics. I. Explicit methods. Computers and Structures 32(6):1371-1386.

El-Sheikh, A. (2000). Approximate dynamic analysis of space trusses. Engineering Structures 22:26-38.

Fox, L., Parker, I.B. (1968). Chebyshev Polynomials in Numerical Analysis, Oxford University Press (London).

Hughes, T.J.R. (1987). The Finite Element Method, Linear Static and Dynamic Finite Element Analysis, Prentice-Hall, Englewood Cliffs (New Jersey).

Lepik, U. (2008). Haar wavelet method for solving higher order differential equations. International Journal of Mathematics and Computation 1:84-94.

Lepik, U. (2009). Haar wavelet method for solving stiff differential equations. International Journal of Mathematics and Computation 14(1):167-181.

Lepik, U. (2005). Numerical solution of differential equations using Haar wavelets. Mathematics and Computers in Simulation 68(2):127-143.

Liu, J.L. (2002). Solution of dynamic response of framed structure using piecewise Birkhoff polynomial. Journal of Sound and Vibration 251(5):847-857.

Mahdavi, S.H., Shojaee, S. (2013). Optimum time history analysis of SDOF systems using free scale of Haar wavelet. Structural Engineering and Mechanics, An International Journal 45(1):95-110.

Mason, J.C., Handscomb, D.C. (2003). Chebyshev Polynomials, Chapman and Hall/CRC.

Rio, G., Soive, A., Grolleau, V. (2005). Comparative study of numerical explicit time integration algorithms. Advances Engineering Software 36:252-265.

Salajeghe, E., Heidari, A. (2006). Time history dynamic analysis of structures using filter bank and wavelet transform. Computers and Structures 83(1):53-68.

Torri, A.J., Machado, R.D. (2012). Structural dynamic analysis of time response of bars and trusses using the generalized finite element method. Latin American Journal of Solids and Structures 9(3):1-31.

Wilson, E.L., Farhoomand, I., Bathe, K.J. (1973). Nonlinear dynamics analysis of complex structures. Earthquake Engineering and Structural Dynamics 1:241-252.

Yuanlu, L. (2010). Solving a nonlinear fractional differential equations using Chebyshev wavelet. Communications in Nonlinear Science and Number Simulation 15(9):2284-2292.